OPEN

PRS GLOBAL OPEN

EXPERIMENTAL

A Novel, Sterilized Microvascular Tissue Product Improves Healing in a Murine Pressure Ulcer Model

Jeffrey M. Gimble, MD, PhD*†
Trivia Frazier, PhD*†
Xiying Wu, MD*
Andrea Alarcon Uquillas, BS*
Claire Llamas, BS†
Theodore Brown, BS, MS†
Doan Nguyen, PhD‡
H. Alan Tucker, BS†
Douglas M. Arm, PhD§
Dale R. Peterson, PhD§
Bruce A. Bunnell, PhD†

Background: Processed microvascular tissue (PMVT), a human structural allograft, is derived from lyophilized human tissue containing microcirculatory cellular components. Since PMVT serves as a source of extracellular matrix (ECM), growth factors, cytokines, and chemokines modulating angiogenesis, inflammation, apoptosis, and endogenous cell recruitment, we hypothesized its application would accelerate wound regeneration in a validated pressure ulcer (PU) model developed in C57BL/6 mice using two 24-hour cycles of skin ischemia/reperfusion created by placement and removal of external magnets.

Methods: Two identical PU injuries (n = 50 female mice) were treated with (a) topical particulate PMVT, (b) injected rehydrated PMVT, or (c) saline control injection, and assessed daily for closure rates, scab formation/removal, and temperature. A baseline control cohort (n = 5) was euthanized at day 0 and treatment group cohorts (n = 5) were killed at 3, 7, or 14 days postinjury. The PU injuries were collagenase-digested for flow cytometric analysis of inflammatory, reparative, and stem cell frequencies and analyzed by hematoxylin and eosin (H&E) histology and immunofluorescence.

Results: PMVT-accelerated wound closure, most notably, topical PMVT significantly increased mean closure from d5 (13% versus -9%) through d13 (92% versus 38%) compared with phosphate-buffered saline (PBS) controls ($P < 0.05$). PMVT also hastened scab formation/removal, significantly accelerated disappearance of inflammatory myeloid (CD11b+) cells while upregulating α-smooth muscle actin, vascular endothelial growth factor A, and placental growth factor and raised skin temperature surrounding the PU site, consistent with increased blood flow.

Conclusions: These results indicate that PMVT has potential as an advanced treatment for restoring normal tissue function in ischemic wounds and merits clinical study. *(Plast Reconstr Surg Glob Open 2018;6:e2010; doi: 10.1097/GOX.0000000000002010; Published online 21 November 2018.)*

INTRODUCTION

The number of individuals at risk for pressure ulcers is expected to increase considerably in the coming decades, due to an increase in life expectancy in the United States and abroad. In developed countries, up to 18% of nursing home residents suffer from pressure ulcers and the resulting hospital costs can account for up to 4% of a nation's health care budget.[1–3] Current standard of care for pressure ulcer/injuries relies on prevention, surgical debridement, skin flaps, negative pressure wound vacuums, acellular dermal grafts or bandages, and topical application of platelet-derived growth factor (PDGF).[4–9] The latter therapy, marketed under the trade name Regranex, is approved by the Food and Drug Administration, but is accompanied by a "Black Box" warning label due to the growth factor's association with increased cancer risk.[10] Thus, there remains a pressing need for more efficacious and economical therapeutic options to improve the quality of life for pressure injury patients and to relieve the resulting societal healthcare burden.

*From the *LaCell, New Orleans, La.; †Center for Stem Cell Research & Regenerative Medicine, Tulane University School of Medicine, New Orleans, La.; ‡Ochsner Medical Center, New Orleans, La.; and §MicroVascular Tissues, Inc., San Diego, Calif.*

Received for publication June 14, 2018; accepted September 17, 2018.

LaCell LLC, 1441 Canal Street, Suite 304, New Orleans, LA 70112 US, jeffrey.gimble@lacell-usa.com

DOI: 10.1097/GOX.0000000000002010

Disclosure: *DMA and DRP are employees of MicroVascular Tissues, Inc. (MVT). MVT sponsored this study and paid for the Article Processing Charges. AA and TF were employees of LaCell LLC at the time of this work; XW and JMG are co-owners and members of LaCell LLC.*

Supplemental digital content is available for this article. Clickable URL citations appear in the text.

Preclinical rodent studies conducted by multiple laboratories, including our own, have demonstrated that cyclic, localized ischemia and reperfusion created by exposure to magnets most closely mimics the human pressure ulcer condition.[11–16] These models have been used successfully to demonstrate the utility and efficacy of cell injections or topical application of cytokines to accelerate and enhance the rate of wound healing in the rodent model. The injection of syngeneic murine adipose-derived stromal/stem cells (ASC) into the base of pressure ulcers has been found to accelerate wound closure rates by up to 2 days in both young (2–4 month) and old (22–24 month) female C57BL/6 mice.[13,14] Such cell-based therapies, by implanting a living cell that can persist for an extended period of time, offer the advantage of continuous delivery of secreted factors at the site of injury. Nevertheless, the regulatory approval process for cell therapy approaches is complex. In addition, cell therapeutic products are subject to extensive lot release criteria that may include tests of bacterial, endotoxin, and viral contamination, functionality, surface immunophenotype, and viability.[17]

As an alternative to live cells, multiple independent teams are exploring cell and tissue-derived products.[18–25] Investigators have begun to use purified cell-derived exosomes and tissue-derived extracellular matrix products as substitutes for live cells in wound repair models. The current study sought to extend this body of literature by evaluating the efficacy of a processed microvascular tissue (PMVT) product. PMVT is a proprietary, aseptically processed, lyophilized, and sterilized human tissue-derived product manufactured by MicroVascular Tissues, Inc. under the trade name of mVASC. It is obtained, processed, and distributed in compliance with current Good Tissue Practices and regulated by Food and Drug Administration as a human tissue intended for transplantation. Both in vivo and in vitro quantitative parameters were used to characterize the temporal kinetics and histology of pressure ulcers in a murine ischemia/reperfusion injury model.

METHODS

Animal Welfare

This study was performed under a protocol entitled "Adipose-Derived Stromal/Stem Cell Therapy for Pressure Ulcers" (4303R) approved by the Tulane University Institutional Animal Care and Use Committee (May 31, 2016). C57BL/6 female (6–8 week old) mice were purchased from Charles River Laboratories (MA) and housed in the Vivarium of the Tulane University School of Medicine Department of Comparative Medicine with routine veterinary oversight. Euthanasia was performed in accordance with Association for Assessment and Accreditation of Laboratory Animal Care (AAALAC)-approved methodologies (CO_2 asphyxiation with secondary thoracic incision).[26]

Wound Induction

The pressure ulcer model used was previously reported, and this study was conducted with slight modifications to adjust for PMVT therapy.[13,14] Briefly, mice were placed under anesthesia using a mixture of isoflurane and oxygen delivered by mask, and the hair on the dorsum was shaved. The dorsal skin was gently pulled up and placed between 2 circular 12-mm diameter magnets (Master Magnetics, Inc., Castle Rock, CO, http://www.magnetsource.com) for 12 hours and removed for 12 hours for 1 ischemia-reperfusion (IR) cycle. Mice were exposed to 2 IR cycles, corresponding to day -2 and day -1, respectively, resulting in 2 wounds per mouse after 2 days of induction. Day 0 corresponds to the first day following the completion of the IR and is used as the starting point for the remainder of the study dates listed below (day 1 to 14).

Wound Healing Treatment and Evaluation

The 3 groups (n = 15 mice per cohort) within the study were PMVT delivered by injection, topical application of PMVT, and phosphate-buffered saline (PBS) injection as a control. For the 2 injection groups, wounds were treated by direct injection of 0.25 ml of the resuspended PMVT product (PMVT1) or PBS control per individual wound site on the immediate day following the completion of the ischemia reperfusion (day 0). PMVT was resuspended at the time of injection by adding 0.5 ml of water to 1 vial. Injections were performed with a 19-gauge needle. For the topical PMVT group, wounds were treated by topical placement of half a vial of the lyophilized PMVT product directly to each individual wound bed (PMVT2) 2 days following the ischemia reperfusion induction (day 2). Wounds in all 3 experimental arms were covered with Adaptic Touch dressings. For topical application, each vial of PMVT was opened and the lyophilized product removed, weighed, and separated into 2 equal amounts. The PMVT2 treatment was delayed 1 day relative to PMVT1 to allow for sufficient exudate release within the wound bed to insure application of the topical powder. Wounds were assessed daily for size and closure. The wound closure was assessed relative to the size/area of the wound at day 2 (2 days following ischemia/reperfusion), which was defined as "0%" closure. The mice were monitored daily by researchers until the day of sacrifice (groups of n = 5 mice per cohort were euthanized on days 3, 7, or 14 following the completion of ischemia reperfusion). A digital carbon fiber caliper (Thermo Fisher Scientific) was positioned at the borders of the wounds to measure the length and width of each wound. Wound size was calculated based on the area of an ellipse = Radius of the length × Radius of the width × π (3.14). On the day of sacrifice, mice were euthanized by CO_2 asphyxiation.

Flow Cytometry

The expression profile of surface antigens was assessed between the treatment groups by flow cytometry at day 3, 7, and 14 following pressure ulcer induction in dermal cells released by collagenase digestion (Figs. 1, 2). As an additional control, tissue from wounds harvested at day 0 (immediately following the completion of the ischemia reperfusion cycles; D0 control) was examined (cohort of n = 5 mice). At each time point, sections of the wound tissue were digested at 37°C with collagenase type I overnight, the isolated cells were fixed and stained with fluorochrome-labeled antibodies directed against

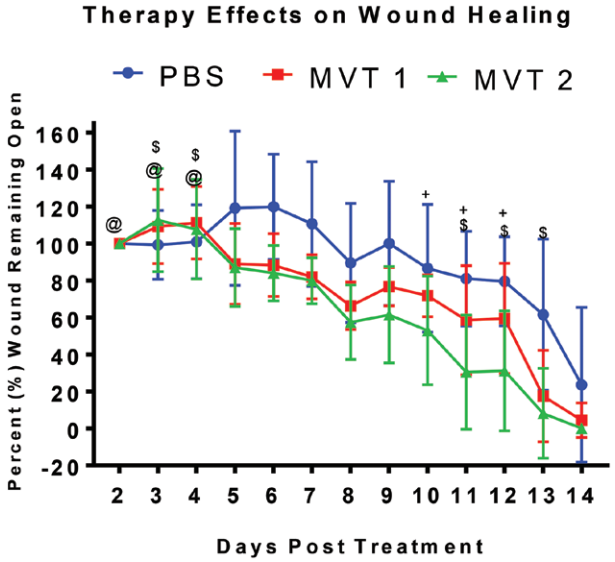

Fig. 1. Therapy effects on wound closure: the experimental cohorts (n = 5 animals each) were monitored daily for wound closure based on photographic measurements. The percentage rate of wound healing was determined relative to the wound size as measured on day 2 posttreatment, which was defined as 100 % wound area (or maximal size of wounding). The healing rate percentages are reported as the mean ± SD. Statistical significance ($P < 0.05$) was determined by Student's *t* test and is indicated by "@" for MVT1 vs PBS control, "$" for MVT2 vs PBS control and "+" for MVT2 vs MVT1.

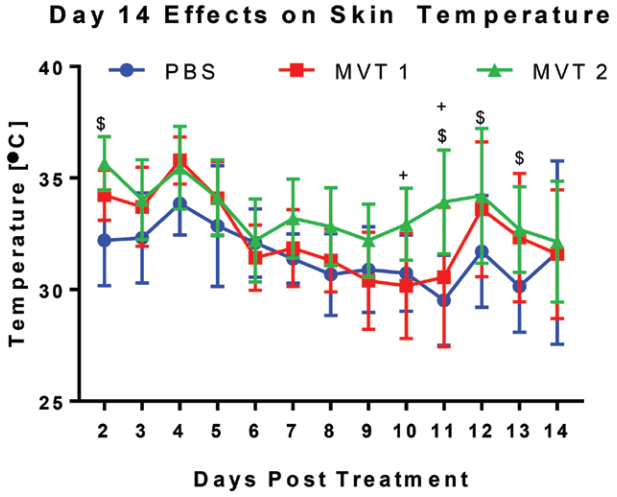

Fig. 2. Day 14 effects on skin temperature: the experimental cohorts (n = 5 animals each) were monitored daily for skin temperature at the pressure ulcer site. Temperature values are reported as the mean ± SD. Statistical significance ($P < 0.05$) was determined by Student's *t* test and is indicated by "$" for MVT2 (topical therapy) vs PBS control and by "+" for MVT2 vs MVT1 (injections).

the surface antigens of interest (Table 1), and the cells were subsequently analyzed by flow cytometry for detection of surface antigens. Flow cytometry was performed using a Galios Flow Cytometer (Beckman Coulter, Brea, Calif.) and analyzed with Kaluza software (Beckman Coulter); a minimum of 5,000 events were collected for each sample.[27]

Paraffin Embedding and Immuno Detection

In parallel, tissues surrounding the pressure ulcer wounds were dissected and fixed in formalin for paraffin embedding and sectioning.[13,14] Tissue at the wound site including a 5 mm rim of unwounded skin was removed and placed in 10% neutral buffered formalin for a minimum of 24 hours. Samples were processed and paraffin embedded. Slides from these paraffin blocks were deparaffinized in xylene (Fisher Scientific, HistoPrep) and rehydrated through graded ethanol washes (Fisher Scientific, HistoPrep). Heat-induced antigen retrieval was performed using a vegetable steamer. Incubation time in heat-induced

Table 1. Antibodies for Immunofluorescence

Antigen	Catalogue #	Ab Source/Type	Dilution
PLGF	Abcam ab196666	rabbit polyclonal	1:200
VEGFA	Abcam ab52917	rabbit monoclonal	1:200
PDGF-BB	Abcam ab23914	rabbit polyclonal	1:500
SDF1	Abcam ab18919	rabbit polyclonal	1:50
alphaSMA	Abcam ab5694	rabbit polyclonal	1:300
Angiopoietin 1	Abcam ab94684	rabbit polyclonal	1:100
NSE	Abcam ab53025	rabbit polyclonal	1:250
CD31	Abcam ab124432	rabbit polyclonal	1:1,000
VEGF receptor 2	Abcam ab45010	rabbit polyclonal	1:25
PDGF receptor β	Abcam ab32570	rabbit monoclonal	1:50
Ankyrin G	NeuroMab, clone N106/65,73-147	mouse monoclonal supernatant	1:5
Tubulin β3	Santa Cruz Biotech SC-51670	mouse monoclonal	1:200
NFH	Proteintech 21471-1-AP	rabbit polyclonal	1:100
F4/80	Cell Signaling Technologies #70076T	rabbit monoclonal	1:250
foxp3	Cell Signaling Technologies #12653	rabbit monoclonal	1:100
Substance P	Abcam ab10353	guinea pig monoclonal	1:200
goat anti-rabbit IgG H&L Alexafluor 488	Abcam ab150077		1:1,000
goat anti-guinea pig IgG H&L alexa fluor 488	Abcam ab150185		1:1,000
goat anti-mouse IgG2b Alexa Fluor 647	ThermoFisher A21242		1:800
goat anti-mouse IgG H&L Alexa Fluor 568	ThermoFisher A11031		1:1,000
goat anti-rabbit IgG H&L Alexa Fluor 488	ThermoFisher A11034		1:1,000
normal goat serum, 50 ml	Abcam ab7481		

NSE, neuron-specific enolase.

antigen retrieval buffer started once buffer reached a temperature of 95°C. After incubation, slides were removed from steamer and the buffer allowed to cool for 20 minutes at room temperature. Slides were then rinsed in running tap water for 10 minutes followed by a 5-minute wash in 1× Tris Buffered Saline, pH 7.6 (TBS). Slides were removed and area around tissue sections was dried using a KimWipe. Sections were encircled using an ImmEdge wax pen (Vector Laboratories, Inc., Burlingame, CA, USA). If needed, permeabilization buffer was applied to each tissue section. Slides were washed in 2–5 minute washes in TBS-T (0.05% Tween-20 in TBS) then blocked in a wash of blocking solution (10% normal goat serum, 1% bovine serum albumin in TBS-T) for 1 hour at room temperature. Primary antibody (Table 1) was applied and slides were stored in a humidifying chamber overnight in the dark at 4°C. On the second day, slides were washed in TBS-T and incubated with the secondary antibody for 1 hour at room temperature. Slides were washed in TBS and coverslipped using Vectashield DAPI mounting media (Vector Labs). Immunofluorescent detection at 10× or 20× magnification was performed using a Leica DMRXA2 deconvoluted fluorescence microscope. As controls for immunofluorescence and immunohistochemistry, brain tissues were harvested and fixed in formalin for paraffin embedding and sectioning as required.

Cell Profiler

The image analysis software CellProfiler 3.0 was used to analyze fluorescent images taken with a deconvoluted microscope at a 10× or 20× magnification.[28] To analyze the images, a pipeline was created in CellProfiler to convert the fluorescent images into binary images and to identify and quantify the number of nuclei present, the area of the image occupied by the protein of interest, and the total area of the image. Images for each antibody in question were analyzed separately from each other. The data obtained from the program were exported to an Excel spreadsheet and arranged based on antibody, group (PMVT1, PMVT2, and PBS), and time point (3, 7, 14 days). The ratio of the area occupied by the protein of interest to the area occupied by the nuclei was calculated with the data obtained. Moreover, for each group and time point, the average and SD of these ratios were calculated. The calculations were analyzed to determine the presence of outliers. It was determined that images containing fewer than 75 nuclei behaved as outliers. A new calculation for the averages and SDs excluding the outliers was performed. *t* Tests were calculated to compare the data relative to day 3, to PMVT1, and to PBS. Excel's Analysis Tool Pack was used to perform all the *t* tests. A bar graph was created for the data obtained for each antibody showing the statistical significant difference determined by *P* values ($P < 0.05$).

Statistical Analyses

The values are presented as means ± SD for in vitro analyses or means ± SEM for in vivo analyses. The statistical differences among 2 or more groups were determined by analysis of variance, followed by post hoc Tukey's multiple comparison tests. Statistical significance was performed using Prism 6.0 (GraphPad Software, Inc., San Diego, Calif., http://www.graphpad.com) or Excel (Microsoft, Redmond, Wash.).

RESULTS

Healing Morphology and Rate: Wound Closure

The dimensions of the wound were monitored visually by photography and converted to areas based on an elliptical shape. Although the absolute initial size of the wounds was larger at early time points in the injected (PMVT1) and topical (PMVT2) conditions, the rate of wound healing displayed a trend toward acceleration with both PMVT therapies relative to the PBS injection control (Fig. 3). There was a significant difference in wound closure percentage between the PMVT treatments and PBS controls through day 13. Most notably, topical PMVT significantly increased mean closure from day 11 through day 13 compared with PBS controls. In addition, there was a significant difference between the injected and topical PMVT therapies, beginning at day 10.

Healing Morphology and Rate: Skin Temperature

The skin temperature measured on the PMVT topical therapy over the pressure ulcer site was generally elevated throughout the study duration compared with the PBS injection control and significantly elevated at both early and late time points (Fig. 4). In contrast, although the PMVT injection therapy showed a trend of elevated temperature compared with the PBS control at early and late time points, there was no significant difference between them.

Healing Morphology and Rate: Eschar Removal

Figure 5 reflects the number of eschars/scabs that fell off posttherapy within the 14-day study. By day 14, 40% of eschars fell off the wounds in the PBS control, 70% in PMVT1, and 100% in PMVT2 cohorts. The existing literature documenting the scab removal timing in pressure ulcer models is limited at best; this has not been a parameter monitored previously to our knowledge.

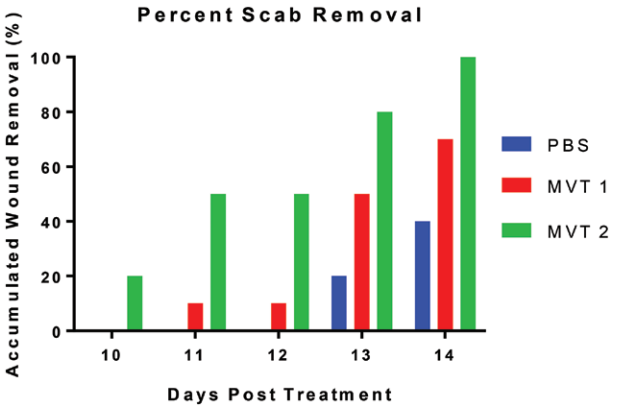

Fig. 3. Percent scab removal: The experimental cohorts (n = 5 animals each) were monitored daily for the removal of the scab or eschar from the site of the pressure ulcer. The percentage of each cohort with scab removal at days 10–14 posttreatment are reported.

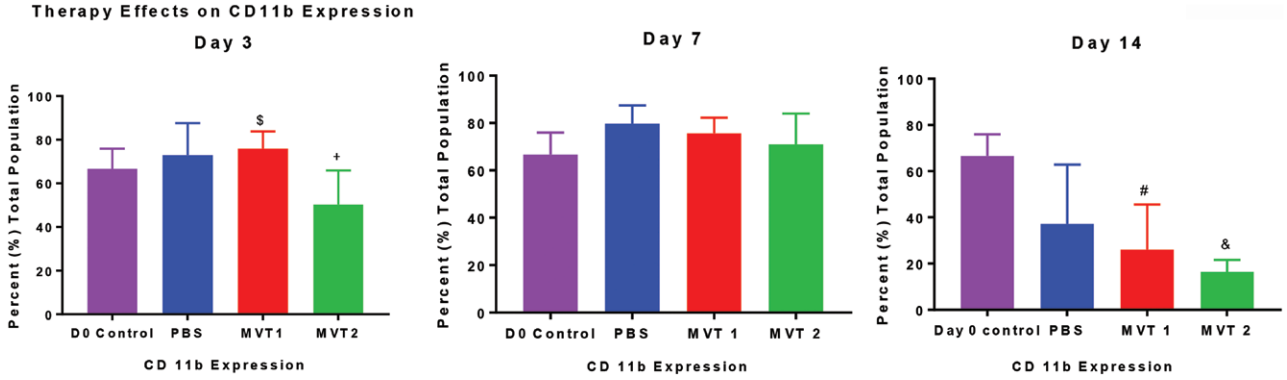

Fig. 4. Fluorescence-Activated Cell Sorting (FACS) profile: The detection of CD11b cell surface antigens on total cells isolated by collagenase digestion from the pressure ulcers at days 3, 7, and 14 posttreatment were determined by flow cytometry. The means ± S.D. of n = 5 animals per cohort are reported. Statistical significance ($P < 0.05$) was determined by Student's *t* test and is indicated by "$" for MVT2 vs PBS control, "+" for MVT2 vs MVT1, "#" for day 0 vs MVT1, and "&" for day 0 vs MVT2.

We presume that the eschar removal reflects the epithelialization of the underlying wound and processes associated with wound healing and closure. Although further work will be required to validate this hypothesis and to explore underlying mechanism, we will continue to evaluate this parameter in future studies.

Flow Cytometric Antigen Profiles

The level of CD11b displayed the most pronounced significant differences as a function of days following pressure ulcer induction and therapy (Fig. 1). Relative to the day 0 conditions, the PBS treated controls showed a nonstatistically significant reduction in CD11b levels only on day 14 following treatment without any significant difference at days 3 or 7. In contrast, on day 14, the CD11b was significantly reduced in the PMVT1 injection groups relative to day 0 controls; however, the relative difference between PBS and PMVT1 treatments was not statistically significant. The most noteworthy impact was observed with PMVT2 topical therapy, in which the level of CD11b was significantly reduced on day 3 and day 14 relative to both the day 0 and PBS treated groups. The next most robust changes were observed for CD146 (Fig. 2). Relative to day 0, the CD146 expression level in the PBS-treated group was significantly reduced at day 3 and day 14 but not on day 7. On day 3, both PMVT1 and PMVT2 treatment groups were not significantly different than the PBS treatment control; however, on day 7, levels of CD146 were significantly reduced in the PMVT1 and PMVT2 treatment groups relative to the PBS-injected control. On day 14, the PMVT1 levels of CD146 were not significantly different from the PBS treated control while the PMVT2 levels were increased and approached the level displayed in the day 0 control. Relative to day 0 controls at day 3, day 7 and day 14, the PBS treatment displayed significantly reduced levels of multiple leukocyte markers (CD4, CD8, CD14, CD25, CD34, CD127, CD133). The PMVT2 treatment group differed significantly from the PBS controls on day 3 only for expression of CD4, CD25, and CD133. Otherwise, no significant differences between the PBS, PMVT1, and PMVT2 treatments were detected at day 7 or day 14.

Immunohistochemistry

Tissues harvested on days 3, 7, and 14 following ischemic injury were fixed and sectioned before immunohistochemical or immunofluorescence analyses with a panel of antibodies detecting cytokines/growth factors, surface antigens, and receptors (**see figure, Supplement Digital Content 1**, which displays immunofluorescence, ***http://links.lww.com/PRSGO/A921***). The area of the cell stained with antibody to each antigen was normalized relative to the nuclear area stained with Hoescht dye using scans from a mean of 11.4±3.7 images at 20× magnification. Relative to the PBS-treated controls at day 3, only the levels of α smooth muscle actin (αSMA) and platelet derived growth factor subunit B were induced with PMVT2 but not PMVT1 treatment. Additionally, both PMVT1 and PMVT2 displayed a trend toward induction of glial fibrillar acidic protein relative to PBS treatment, although this did not achieve statistical significance. By day 7, both PMVT1 and PMVT2 significantly induced the levels of αSMA and stromal derived factor 1 (SDF1) relative to PBS treatment. Additionally, PMVT1 significantly decreased Ankyrin G (AnkG) while PMVT2 significantly decreased vascular endothelial growth factor A (VEGFA) relative to PBS treatment. By day 14, both PMVT1 and PMVT2 significantly increased expression of SDF1 and VEGFA relative to PBS treatment while only PMVT2 induced the level of platelet derived growth factor subunit B. Although levels of β3 tubulin and neurofilament heavy chain (NFH) did not achieve statistical significance relative to time matched PBS treated controls, PMVT1 showed a pattern of increased expression for β3 tubulin at day 3 and increased expression for NFH at day 7. In contrast, the levels of CD31, placental growth factor, PDGF receptor β (PDGFRβ), F4/80, Ankyrin B, and VEGF receptor 2 were not significantly different between PBS treatment and either PMVT1 or PMVT2 treatments at any time during the study period.

DISCUSSION

In the coming decade(s), the demographic of aged individuals in the United States and internationally will

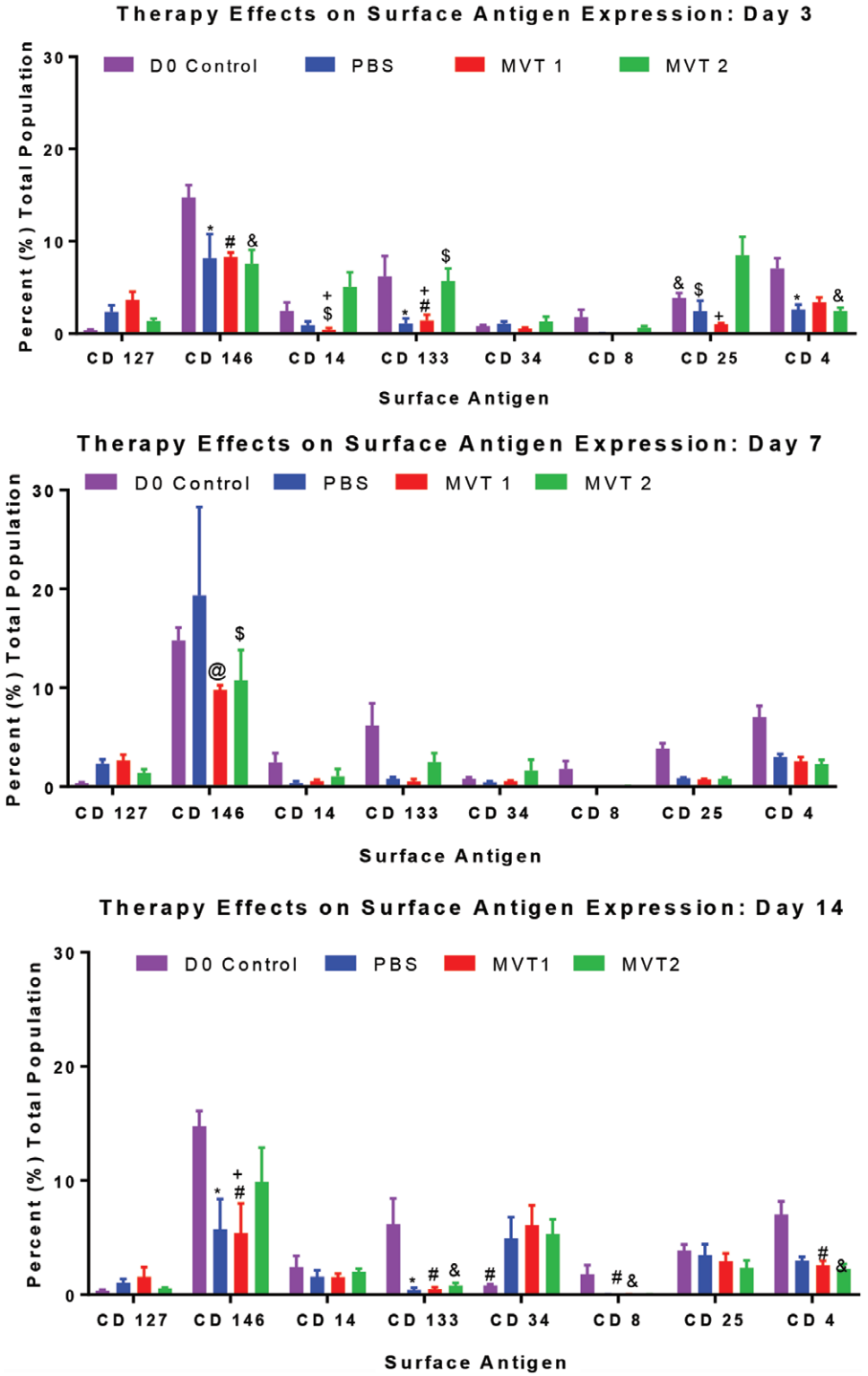

Fig. 5. FACS profile: The detection of CD133, CD34, CD146, CD14, CD127, CD25, CD4, and CD8 cell surface antigens on total cells isolated by collagenase digestion from the pressure ulcers at days 3, 7, and 14 posttreatment were determined by flow cytometry. The means ± S.D. of n = 5 animals per cohort are reported. Statistical significance ($P < 0.05$) was determined by Student's *t* test and is indicated by "$" for MVT2 vs PBS control, "+" for MVT2 vs MVT1, "#" for day 0 vs MVT1, and "&" for day 0 vs MVT2.

account for a far greater percentage of the overall population. These individuals are at considerable risk for the development of pressure injuries during their lifetime. Indeed, the risk increases considerably upon confinement to nursing homes or assisted care residences. Consequently, pressure ulcers will continue to be a leading cause of morbidity and mortality and will drain resources from each nation's healthcare economy. The current data derived from a murine skin model of pressure injury demonstrate that PMVT, delivered either by local injection or topically, will accelerate and enhance the rate of wound closure and eschar removal. This correlates with increased level of expression of proteins associated with angiogenesis and vascularity and the homing of reparative and regenerative cells to the site of injury. Flow cytometric studies indicate that the application of PMVT accelerates a reduction in the number of $CD11b^+$ myeloid cells remaining within the pressure ulcer site 14 days following the injury. Although these findings are correlative, they suggest that the PMVT acts mechanistically through the induction of cytokine/growth factors promoting angiogenesis (PDGFβ, VEGFα) and stromal/stem cell homing (SDF1) at the site of ischemic injury. The early (day 3) trend toward PMVT induction of glial fibrillar acidic protein, a biomarker detected on the surface of nonmyelinated and proliferating Schwann cells, is consistent with ongoing reparative processes. Likewise, the decrease of AnkG at day 7 suggests injection of PMVT may have a beneficial effect in reducing pressure ulcer-related pain. Additionally, the patterns of β3 tubulin and NFH following PMVT1 treatment are consistent with axonal repair and regeneration. Further studies will be necessary to determine the factors within PMVT that account for the modulation of these regenerative biochemical pathways.

Previous studies in the literature have examined cell- and tissue-derived therapies in murine wound healing models and obtained similarly promising results. The injection of syngeneic murine ASC into a murine pressure ulcer model demonstrated that the ASC accelerated repair and regeneration in dose- and time-dependent manner.[13,14] The transplanted cells integrated and persisted in the wound site for up to 20 days postinjury and contributed, in part, through their integration into the dermal and adipose layers. Improved recovery was associated with increased expression of cytokines and enzymes associated with extracellular matrix remodeling, such as transforming growth factor β and matrix metalloproteinases.[13,14] Clinical studies (n = 10 patients) by Carstens et al.[29] determined that the localized injection of autologous human adipose-derived stromal vascular fraction (SVF) cells around the vessels and diabetic foot ulcers improved vasculogenesis and resulted in limb salvage in patients with ischemic lower extremities at high risk of amputation. It is noteworthy that SVF cells are an abundant source of pericytic cells, reflecting the microvascular nature of adipose tissue.[30–32] In a similar sized clinical study (n = 20 patients), Cervelli et al.[33] determined that either autologous human SVF cells or autologous fat grafting supplemented with platelet rich plasma improved the reepithelialization rate of lower extremity ulcers secondary to trauma. In a larger cohort (n = 223 patients), this same group has reported improved fat volume retention and wound repair when using platelet rich plasma enhanced fat grafting or lipotransfer in patients with ulcers or related soft-tissue defects.[34] To complement these reports, there is a growing body of literature indicating that adipose-derived cells and tissue exert regenerative properties through their secretion of exosomes containing cytokines/growth factors, antioxidants, and microRNAs.[18,35,36] It remains to be determined if such regenerative factors can be concentrated, isolated, and preserved for later delivery as a substitute for live cell or tissue transfer. One or more of these agents could be responsible for the wound healing enhancement exerted by PMVT. Regardless, this published body of work demonstrate the presence of reparative factors in microvascular-derived cells or tissues capable of accelerating recovery in animal skin wound models and human lower extremity ulcers secondary to ischemia.

There are several potential limitations to the current article and its study design. First, the study has employed a murine skin wound ischemia reperfusion model of pressure injury. Although this model has been validated in multiple publications,[12–15,37–39] the translatability of findings in a murine skin model to the human condition faces some challenges. Rodent skin healing occurs in part due to contraction rather than reepithelialization. Some investigators have advocated the placement of a silicon ring around murine full thickness injury models to mitigate the contribution of contracture to the rate of wound closure[40,41]; however, others have questioned the need for splinting and present data in 3 different murine strains indicating that contracture accounts for, at most, 40–50% of the healing rate.[42] Consequently, the model employed in the current article remains both appropriate and valid. Nevertheless, the reliance on monitoring of the skin surface temperature and rate of eschar removal are limited outcome parameters due to the absence of similar evaluations in the literature. It would be desirable to include noninvasive evaluation of blood flow by laser Doppler or pulse oximetry measurements in future studies. A second limitation of the current study is its reliance on a single sex (female) and dosage and the analysis of a restricted number of time points over a 2-week healing period. To address this concern, future studies will need to include both male and female mice, a dose curve response, and a more expanded time course of repair. A third limitation is that this proof of principle pilot study was strategically restricted to focus on otherwise healthy, immunocompetent young mice as previously published.[13,14] Nevertheless, it is well established that metabolic disease status, such as a diabetic *db/db* background or advanced age modulate skin wound healing.[13,43] Further studies evaluating the impact of the PMVT product in either the *db/db* or aged mouse model is warranted. A fourth limitation is the study's reliance on quantitative analysis of immunofluorescent detection of relevant proteins. Since such quantitative metrics are a relatively new measurement made possible by advanced imaging software, it would be advantageous to include alternative established assays such as qRT-PCR or western immunoblots as complementary quantitative

outcome measures. Finally, in addition to these limitations, another unanswered question remains, specifically, does the PMVT product contain either exosomes or microRNAs that might contribute to its mechanism of action? Further evaluation of the microRNA and exosome content of the PMVT would address this issue. Together, these limitations remain areas of interest and will be pursued in further analyses that fall beyond the scope of the current article.

In conclusion, the current work documents the ability of PMVT, either topically or by direct injection, to increase the rate of closure, accelerate eschar removal, decrease the myeloid immune response, and increase vascularization of a pressure ulcer injury in female mice. These actions are associated with the increased early and late expression of angiogenic and vasculogenic growth factors. PMVT also modulated T-cell subsets and stem/progenitor cell presence and increased the number of vascular and some neural cell populations in the wound site. Despite any potential limitations, the current data provide a foundation upon which to advance additional mechanistic evaluations of PMVT's underlying actions in support of clinical trials.

Jeffrey M. Gimble, MD, PhD
Center for Stem Cell Research
& Regenerative Medicine
Tulane University School of Medicine
New Orleans, La.
Email: jgimble@tulane.edu

ACKNOWLEDGEMENTS

The authors thank: Gina Dobek, DVM, Department of Comparative Medicine, Tulane University School of Medicine, and the staff of the Tulane University Vivarium for their assistance and dedication to insuring the welfare and care of the laboratory animals employed in this study and; Dina Gaupp of the Histology Core Facility in the Center for Stem Cell Research and Regenerative Medicine for her assistance in processing tissue samples for experimental analyses.

REFERENCES

1. White-Chu EF, Flock P, Struck B, et al. Pressure ulcers in long-term care. *Clin Geriatr Med.* 2011;27:241–258.
2. Flack S, Apelqvist J, Keith M, et al. An economic evaluation of VAC therapy compared with wound dressings in the treatment of diabetic foot ulcers. *J Wound Care.* 2008;17:71–78.
3. Trueman P, Whitehead SJ. The economics of pressure relieving surfaces: an illustrative case study of the impact of high-specification surfaces on hospital finances. *Int Wound J.* 2010;7:48–54.
4. Clemens MW, Broyles JM, Le PN, et al. Innovation and management of diabetic foot wounds. *Surg Technol Int.* 2010;20:61–71.
5. Vangilder C, Macfarlane GD, Meyer S. Results of nine international pressure ulcer prevalence surveys: 1989 to 2005. *Ostomy Wound Manage.* 2008;54:40–54.
6. VanGilder C, Lachenbruch C, Algrim-Boyle C, et al. The International Pressure Ulcer Prevalence™ Survey: 2006-2015: a 10-year pressure injury prevalence and demographic trend analysis by care setting. *J Wound Ostomy Continence Nurs.* 2017;44:20–28.
7. Felder JM 3rd, Goyal SS, Attinger CE. A systematic review of skin substitutes for foot ulcers. *Plast Reconstr Surg.* 2012;130:145–164.
8. Iorio ML, Shuck J, Attinger CE. Wound healing in the upper and lower extremities: a systematic review on the use of acellular dermal matrices. *Plast Reconstr Surg.* 2012;130:232S–241S.
9. Waycaster CR, Gilligan AM, Motley TA. Cost-effectiveness of becaplermin gel on diabetic foot ulcer healing changes in wound surface area. *J Am Podiatr Med Assoc.* 2016;106:273–282.
10. Baldo BA. Side effects of cytokines approved for therapy. *Drug Saf.* 2014;37:921–943.
11. de la Garza-Rodea AS, Knaan-Shanzer S, van Bekkum DW. Pressure ulcers: description of a new model and use of mesenchymal stem cells for repair. *Dermatology.* 2011;223:266–284.
12. Stadler I, Zhang RY, Oskoui P, et al. Development of a simple, noninvasive, clinically relevant model of pressure ulcers in the mouse. *J Invest Surg.* 2004;17:221–227.
13. Strong AL, Bowles AC, MacCrimmon CP, et al. Adipose stromal cells repair pressure ulcers in both young and elderly mice: potential role of adipogenesis in skin repair. *Stem Cells Transl Med.* 2015;4:632–642.
14. Strong AL, Bowles AC, MacCrimmon CP, et al. Characterization of a murine pressure ulcer model to assess efficacy of adipose-derived stromal cells. *Plast Reconstr Surg Glob Open.* 2015;3:e334.
15. Saito Y, Hasegawa M, Fujimoto M, et al. The loss of MCP-1 attenuates cutaneous ischemia-reperfusion injury in a mouse model of pressure ulcer. *J Invest Dermatol.* 2008;128:1838–1851.
16. Peirce SM, Skalak TC, Rodeheaver GT. Ischemia-reperfusion injury in chronic pressure ulcer formation: a skin model in the rat. *Wound Repair Regen.* 2000;8:68–76.
17. Mendicino M, Bailey AM, Wonnacott K, et al. MSC-based product characterization for clinical trials: an FDA perspective. *Cell Stem Cell.* 2014;14:141–145.
18. Maumus M, Jorgensen C, Noël D. Mesenchymal stem cells in regenerative medicine applied to rheumatic diseases: role of secretome and exosomes. *Biochimie.* 2013;95:2229–2234.
19. Brown BN, Freund JM, Han L, et al. Comparison of three methods for the derivation of a biologic scaffold composed of adipose tissue extracellular matrix. *Tissue Eng Part C Methods.* 2011;17:411–421.
20. Choi JS, Kim BS, Kim JY, et al. Decellularized extracellular matrix derived from human adipose tissue as a potential scaffold for allograft tissue engineering. *J Biomed Mater Res A.* 2011;97:292–299.
21. Wang L, Johnson JA, Zhang Q, et al. Combining decellularized human adipose tissue extracellular matrix and adipose-derived stem cells for adipose tissue engineering. *Acta Biomater.* 2013;9:8921–8931.
22. Zhang S, Lu Q, Cao T, et al. Adipose tissue and extracellular matrix development by injectable decellularized adipose matrix loaded with basic fibroblast growth factor. *Plast Reconstr Surg.* 2016;137:1171–1180.
23. Turner AE, Yu C, Bianco J, et al. The performance of decellularized adipose tissue microcarriers as an inductive substrate for human adipose-derived stem cells. *Biomaterials.* 2012;33:4490–4499.
24. Lavoie JR, Rosu-Myles M. Uncovering the secretes of mesenchymal stem cells. *Biochimie.* 2013;95:2212–2221.
25. Kupcova Skalnikova H. Proteomic techniques for characterisation of mesenchymal stem cell secretome. *Biochimie.* 2013;95:2196–2211.
26. *Guide for the Care and Use of Laboratory Animals.* 8h ed.: National Research Council; 2010.
27. Frazier TP BA, Lee S, Abbott R, et al. Serially transplanted nonpericytic CD146- adipose stromal/stem cells in silk bioscaffolds regenerate adipose tissue in vivo. *Stem Cells.* 2016;34(4):1087–1111.
28. Carpenter AE, Jones TR, Lamprecht MR, et al. CellProfiler: image analysis software for identifying and quantifying cell phenotypes. *Genome Biol.* 2006;7:R100.
29. Carstens MH, Gómez A, Cortés R, et al. Non-reconstructable peripheral vascular disease of the lower extremity in ten patients treated with adipose-derived stromal vascular fraction cells. *Stem Cell Res.* 2017;18:14–21.

30. Crisan M, Yap S, Casteilla L, et al. A perivascular origin for mesenchymal stem cells in multiple human organs. *Cell Stem Cell.* 2008;3:301–313.
31. Traktuev DO, Merfeld-Clauss S, Li J, et al. A population of multipotent CD34-positive adipose stromal cells share pericyte and mesenchymal surface markers, reside in a periendothelial location, and stabilize endothelial networks. *Circ Res.* 2008;102: 77–85.
32. Zannettino AC, Paton S, Arthur A, et al. Multipotential human adipose-derived stromal stem cells exhibit a perivascular phenotype *in vitro* and in vivo. *J Cell Physiol.* 2008;214:413–421.
33. Cervelli V, Gentile P, De Angelis B, et al. Application of enhanced stromal vascular fraction and fat grafting mixed with PRP in posttraumatic lower extremity ulcers. *Stem Cell Res.* 2011;6:103–111.
34. Cervelli V, Bocchini I, Di Pasquali C, et al. P.R.L. platelet rich lipotransfert: our experience and current state of art in the combined use of fat and PRP. *Biomed Res Int.* 2013;2013:434191.
35. Katakowski M, Buller B, Zheng X, et al. Exosomes from marrow stromal cells expressing miR-146b inhibit glioma growth. *Cancer Lett.* 2013;335:201–204.
36. Martin EC, Qureshi AT, Dasa V, et al. MicroRNA regulation of stem cell differentiation and diseases of the bone and adipose tissue: perspectives on miRNA biogenesis and cellular transcriptome. *Biochimie.* 2016;124:98–111.
37. Lanzafame RJ, Stadler I, Cunningham R, et al. Preliminary assessment of photoactivated antimicrobial collagen on bioburden in a murine pressure ulcer model. *Photomed Laser Surg.* 2013;31:539–546.
38. Motegi SI, Sekiguchi A, Uchiyama A, et al. Protective effect of mesenchymal stem cells on the pressure ulcer formation by the regulation of oxidative and endoplasmic reticulum stress. *Sci Rep.* 2017;7:17186.
39. Kaneko M, Minematsu T, Yoshida M, et al. Compression-induced HIF-1 enhances thrombosis and PAI-1 expression in mouse skin. *Wound Repair Regen.* 2015;23:657–663.
40. Michaels J 5th, Churgin SS, Blechman KM, et al. db/db mice exhibit severe wound-healing impairments compared with other murine diabetic strains in a silicone-splinted excisional wound model. *Wound Repair Regen.* 2007;15:665–670.
41. Galiano RD, Michaels J 5th, Dobryansky M, et al. Quantitative and reproducible murine model of excisional wound healing. *Wound Repair Regen.* 2004;12:485–492.
42. Chen L, Mirza R, Kwon Y, et al. The murine excisional wound model: Contraction revisited. *Wound Repair Regen.* 2015;23: 874–877.
43. Amos PJ, Kapur SK, Stapor PC, et al. Human adipose-derived stromal cells accelerate diabetic wound healing: impact of cell formulation and delivery. *Tissue Eng Part A.* 2010;16:1595–1606.